Investigation of Electron Temperature Gradient Driven Micro-Reconnecting Modes in Toroidal High-Energy Plasmas

by

Kevin T. Takasaki

Submitted to the Department of Physics
in partial fulfillment of the requirements for the degree of

Bachelor of Science in Physics

at the

MASSACHUSETTS INSTITUTE OF TECHNOLOGY

May 2007
[June 2007]

Author .....
Department of Physics
May 23, 2007

Certified by .....
Bruno Coppi
Professor
Thesis Supervisor

Accepted by .....
David Pritchard
Senior Thesis Coordinator, Department of Physics

Investigation of Electron Temperature Gradient Driven Micro-Reconnecting Modes in Toroidal High-Energy Plasmas

by

Kevin T. Takasaki

Submitted to the Department of Physics
on May 23, 2007, in partial fulfillment of the
requirements for the degree of
Bachelor of Science in Physics

Abstract

Experiments carried out with magnetically confined, high temperature plasmas have revealed important effects that have yet to be justified by existing theory. In particular, there arises an anomalous particle inflow in the central region of the plasma column. Experimental evidence suggests that this particle transport results from the excitation of unstable, short wavelength modes driven by the electron temperature gradient, but the validity of the existing theory is limited to the edge of the plasma column. This thesis investigates the question of how microscopic, electron temperature gradient driven, micro-reconnecting modes may collectively give rise to particle inflow in the central region of the plasma column by examining solutions to the mode dispersion relation. Derivations of micro-reconnecting modes in both fluid and kinetic theory are presented, and the resulting dispersion relation is analyzed.

Thesis Supervisor: Bruno Coppi
Title: Professor

Acknowledgments

The author is indebted and most deeply grateful to Bruno Coppi, Chris Crabtree, Vadim Roytershteyn, and the High-Energy Plasma Physics Group for their generosity, patience, and expertise. Their unwavering support and invaluable assistance taught me all that I know about plasma, and more.

Contents

List of Figures

Chapter 1

Introduction

We begin this chapter with an outline of what will be presented in this thesis. The aim of Chapter 1 is to contextualize the following work by communicating to the reader the importance of anomalous transport processes in fusion-burning plasma research. In the next section, we introduce the topic of controlled thermonuclear fusion, the development of which provides the main impetus for this work.

Chapter 2 introduces the hydrodynamic description of plasma behavior and presents a derivation of micro-reconnecting modes in the fluid approximation. The fluid derivation highlights many of the important orderings which characterize the regime in which we are interested. In Chapter 3, kinetic theory is discussed and a more general derivation of the modes in Chapter 2 is presented. The results of Chapters 2 and 3 are used in Chapter 4 to derive the dispersion relation. Analysis of this dispersion relation in Chapter 4 will allow us to characterize mode stability and discuss the implications of our results.

1.1 Background

The fundamental goal of thermonuclear fusion research is to devise a method by which a plasma may be heated to ignition and confined at sufficiently high density for a sufficiently long duration to satisfy the Lawson criterion. Because fusion-burning plasma must be contained at energies typically in excess of 1 keV, the plasma cannot

be contained by material barriers, and the majority of present day research has focused on the possibility of confining plasma with appropriately tuned magnetic fields.

The confinement scheme in which we are interested is the tokamak. Tokamaks are axisymmetric tori which confine high-energy plasma in a helically winding magnetic field comprised of an externally generated toroidal component and a poloidal component generated by the plasma current itself. Drift effects resulting from spatial curvature and the gradient of the magnetic field necessitate helical winding to suppress instabilities.

Magnetic confinement research has yielded significant advances in the past fifty years, but there remain many experimentally observed phenomena which have yet to be explained by theory. Among these phenomena, magnetic reconnection and anomalous transport processes present a particular challenge to the understanding of plasma behavior and the development of controlled fusion. Magnetic reconnection disturbs the stability of ambient fields by the creation of magnetic islands as depicted in Figure 1-1. These islands join field lines from initially distinct domains and facilitate particle and energy transport across the field.

1.2 Motivation

Previous work performed by Coppi and Spight [5] identified long wavelength, electrostatic ion-mixing modes facilitating the transport of ions and electrons against the density gradient. The magnitude of the inflow depended on the finiteness of the longitudinal electron thermal conductivity which is a characteristic of collisional regimes at the edge of the plasma column. In collisionless regimes, drift-tearing modes were thought to be suppressed by the combined effects of Landau damping and the temperature gradient, but even in experiments with low degrees of collisionality, magnetic reconnection and anomalous transport have been observed [4]. Explaining the mechanism behind the generation of these instabilities would be a significant advance in understanding the behaviors of space and laboratory plasmas.

In this thesis, we consider a class of short-wavelength, electromagnetic modes

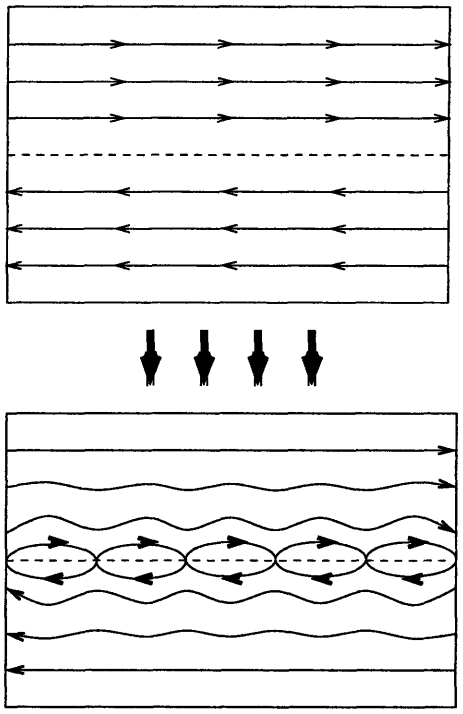

Figure 1-1: Diagram depicting reconnection of field lines and formation of magnetic islands.

driven by the electron temperature gradient and investigate the question of whether these modes, known as micro-reconnecting modes in the literature, could be responsible for the onset of the anomalous drift-tearing mode. These micro-reconnecting modes are called such because they produce magnetic reconnection (islands) and turbulence on distances on the order of the skin depth. It has been postulated [7] that the excitation of a background of microscopic modes may collectively sustain the larger drift-tearing modes which give rise to macroscopic anomalous transport and magnetic reconnection in collisionless regimes. For this to happen, however, these microscopic modes must be driven unstable, and the stability of these modes is what we primarily seek to analyze.

Chapter 2

Fluid Approximation

In this chapter, we discuss the consequences of modelling plasma as an electrically conducting fluid. Applying concepts from fluid mechanics to the particular case of a fluid composed of charged species yields the fluid equations which we may use to describe plasma behavior in the appropriate limit. Using the fluid equations, we derive an equation for the component of the vector potential along the prevailing magnetic field.

2.1 Fluid Equations

The hydrodynamic regime is often characterized by the limit in which the ratio between the mean-free-path of particles and the relevant distance scale under consideration is small, i.e. $\lambda_{mfp} \ll L$. On scales where L dominates λ_{mfp}, collisions occur frequently, and the system quickly settles into local thermodynamic equilibrium. In this case, the system may be considered to populate local micro-states independently and with equal probability, which is to say that the fundamental theorem of statisical mechanics applies. In the hydrodynamic limit, then, the system has well-defined local properties, such as temperature, $T(\mathbf{x}, t)$ (measured in units of energy), density, $n(\mathbf{x}, t)$, and flow velocity, $\mathbf{u}(\mathbf{x}, t)$, which vary smoothly in space and in time. The

local equilibrium is described by a Maxwell-Boltzmann distribution

$$f_M(\mathbf{x}, \mathbf{v}, t) = Cn(\mathbf{x}, t) \exp\left[-\frac{m|\mathbf{v} - \mathbf{u}(\mathbf{x}, t)|^2}{2T(\mathbf{x}, t)}\right] \tag{2.1}$$

in which the local parameters n, $\mathbf{u}$, and T, are determined by conservation laws to be discussed shortly.

In the case of fully ionized plasma, mean-free-paths are typically very long. In this case, a strong external magnetic field must serve to maintain the local Maxwellian distribution and supply the "caging effect" that is characteristic of fluids [8]. The fluid equations are then derived by taking moments of the local distribution, and the derivation can be found in any textbook on the subject. The equations expressing conservation of mass, momentum, and energy, are given by

$$\frac{\partial n}{\partial t} + \nabla \cdot (n\mathbf{u}) = 0 \tag{2.2a}$$

$$mn\left(\frac{\partial}{\partial t} + \mathbf{u} \cdot \nabla\right)\mathbf{u} = nq\left(\mathbf{E} + \mathbf{u} \times \mathbf{B}\right) - \nabla(nT) \tag{2.2b}$$

$$\frac{3}{2}n\left(\frac{\partial}{\partial t} + \mathbf{u} \cdot \nabla\right)T = 0. \tag{2.2c}$$

To linearize the equations in Eq.(2.2), we express the quantities of the plasma as an equilibrium value plus a small perturbation as shown for the quantity, Q, here:

$$Q = Q^{(0)} + \tilde{Q}. \tag{2.3}$$

In the following derivations, we will consider perturbative waves of the form

$$\tilde{Q} = Q^{(1)} \exp\left[i(\mathbf{k} \cdot \mathbf{x} - \omega t)\right]. \tag{2.4}$$

In particular, we are interested in the mode growth which can be identified with the imaginary part of ω.

2.2 Micro-Reconnecting Modes

We now present a fluid derivation [6] of the micro-reconnecting modes. For the following derivation, we refer to a one-dimensional, plane-equilibrium configuration and consider the motion of the electrons in which there is no applied electric field and no particle flow at equilibrium, i.e. $\mathbf{E}^{(0)} = \mathbf{u}_e^{(0)} = 0$. In this case, the equilibrium density and temperature vary appreciably only in one direction which we will take to be $\hat{\mathbf{x}}$. The external magnetic field is composed of a strong axial component with weak shear, as given by

$$\mathbf{B} = B_0 \left[\hat{\mathbf{z}} + \frac{x}{L_s} \hat{\mathbf{y}} \right]. \tag{2.5}$$

The parameter L_s is called the shear length, and we take it to be large compared to the dimensions of the system. The magnetic field described by Eq.(2.5) is useful in investigating microscopic phenomena in toroidal plasmas, as the weak shear model approximates the tokamak field on small distance scales. A graphical picture of the sheared field is shown in Figure 2-1.

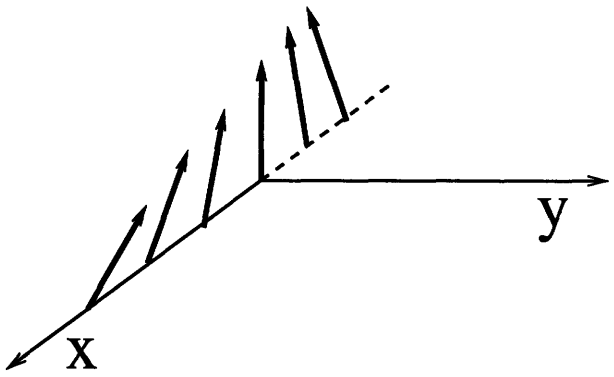

Figure 2-1: Graphic showing the direction of field lines given by Eq.(2.5) in sheared slab geometry.

2.2.1 Parallel Momentum Conservation

Taking the scalar product of Eq.(2.2b) for the electrons with the unit vector $\mathbf{b} = \frac{\mathbf{B}}{B}$, we derive an equation for the component of the electron momentum parallel to the

local magnetic field:

$$m_e n_e \left(\mathbf{b} \cdot \frac{\partial \mathbf{u}_e}{\partial t} + \mathbf{b} \cdot (\mathbf{u}_e \cdot \nabla \mathbf{u}_e) \right) = -\mathbf{b} \cdot \nabla (n_e T_e) - e n_e \mathbf{b} \cdot \mathbf{E}. \tag{2.6}$$

We expand the quantities in Eq.(2.6) with the expression given on the right-hand side of Eq.(2.3). Ignoring higher-order terms, i.e. terms containing products of first-order quantities, we find

$$m_e n_e^{(0)} \mathbf{b}^{(0)} \cdot \frac{\partial \tilde{\mathbf{u}}_e}{\partial t} = -\tilde{\mathbf{b}} \cdot \nabla (n_e^{(0)} T_e^{(0)}) - \mathbf{b}^{(0)} \cdot \nabla (\tilde{n}_e T_e^{(0)}) - \mathbf{b}^{(0)} \cdot \nabla (n_e^{(0)} \tilde{T}_e) - e n_e^{(0)} \mathbf{b}^{(0)} \cdot \tilde{\mathbf{E}}. \tag{2.7}$$

We would like to express $\tilde{\mathbf{b}}$ in terms of the perturbed vector potential $\tilde{\mathbf{A}}$. We note that $\mathbf{B} = \nabla \times (\mathbf{A}^{(0)} + \tilde{\mathbf{A}})$ and $\mathbf{B}^{(0)} = \nabla \times \mathbf{A}^{(0)}$. We then find that

$$\tilde{\mathbf{B}} = \nabla \times \tilde{\mathbf{A}} = \nabla \tilde{A}_{||} \times \mathbf{b}^{(0)} + \tilde{A}_{||} \nabla \times \mathbf{b} + \nabla \times \mathbf{b}^{(0)} + \nabla \times \tilde{\mathbf{A}}_{\perp}. \tag{2.8}$$

Recalling that $\mathbf{b} = \mathbf{B}/B$ and $\mathbf{B} = \mathbf{B}^{(0)} + \tilde{\mathbf{B}}$, we find that

$$\begin{aligned}
\mathbf{b} &= \frac{\mathbf{B}^{(0)} + \tilde{\mathbf{B}}}{\left[(B^{(0)})^2 + 2\mathbf{B}^{(0)} \cdot \tilde{\mathbf{B}} \right]^{1/2}} \\
&\simeq \frac{\mathbf{B}^{(0)} + \tilde{\mathbf{B}}}{B^{(0)}} \left[1 - \frac{\mathbf{B}^{(0)} \cdot \tilde{\mathbf{B}}}{(B^{(0)})^2} \right] \\
&= \frac{\mathbf{B}^{(0)}}{B^{(0)}} + \frac{\tilde{\mathbf{B}} - \mathbf{b}^{(0)} (\mathbf{b}^{(0)} \cdot \tilde{\mathbf{B}})}{B^{(0)}} \\
&= \mathbf{b}^{(0)} + \frac{\tilde{\mathbf{B}} - \tilde{B}_{||} \mathbf{b}^{(0)}}{B^{(0)}}.
\end{aligned}$$

In the low-β limit, the diamagnetic effect arising from $\tilde{\mathbf{A}}_{\perp}$ is negligible. Thus, we find

$$\tilde{\mathbf{b}} \simeq \frac{\tilde{\mathbf{B}}}{B^{(0)}} \tag{2.9}$$

Henceforth, we will drop the superscript $^{(0)}$ from equilibrium quantities for notational simplicity. Here, we express the perturbed electric field in Eq.(2.7) as $\tilde{\mathbf{E}} = -\nabla \tilde{\Phi} - \frac{1}{c} \frac{\partial \tilde{\mathbf{A}}}{\partial t}$. Given Eq.(2.4), the equilibirum neutrality condition, $n_e = n_i = n$, and the

plane configuration ($\mathbf{b}\cdot\nabla T_e = 0$ and $\mathbf{b}\cdot\nabla n = 0$) from the definition of the problem, we find Eq.(2.7) becomes

$$-i\omega m_e n\tilde{u}_{e||} = -n\tilde{b}_x\frac{dT_e}{dx} - T_e\tilde{b}_x\frac{dn}{dx} - T_e\mathbf{b}\cdot\nabla\tilde{n}_e - n\mathbf{b}\cdot\nabla\tilde{T}_e + en\left(\mathbf{b}\cdot\nabla\tilde{\Phi} - i\frac{\omega}{c}\tilde{A}_{||}\right) \quad (2.10)$$

where $\tilde{b}_x = \tilde{\mathbf{b}}\cdot\hat{\mathbf{x}}$ and $\tilde{u}_{e||} = \tilde{\mathbf{u}}_e\cdot\mathbf{b}$. Neglecting $\tilde{\mathbf{A}}_\perp$ in Eq.(2.9), we can show

$$\tilde{b}_x \simeq \frac{\nabla\tilde{A}_{||}\times\mathbf{b}}{B}\cdot\hat{\mathbf{x}}. \quad (2.11)$$

In the plane equilibrium configuration we are considering, perturbations propagate in the $\hat{\mathbf{y}}$ and $\hat{\mathbf{z}}$directions, i.e. $\mathbf{k} = k_y\hat{\mathbf{y}} + k_z\hat{\mathbf{z}}$ in Eq.(2.4). Here, we introduce the wave vector component along the field

$$k_{||} \equiv \mathbf{k}\cdot\mathbf{b} = k_y b_y + k_z b_z.$$

and the following parameters:

$$\omega_{*Te} \equiv -\frac{k_y c}{eB}\frac{dT_e}{dx}$$

is the drift frequency associated with the electron temperature gradient and

$$\eta_e \equiv \left(\frac{1}{T_e}\frac{dT_e}{dx}\right)\left(\frac{1}{n}\frac{dn}{dx}\right)^{-1}$$

measures the ratio of the strengths of the temperature and density gradients. For micro-reconnecting modes driven by the electron temperature gradient, we assume the orderings $\eta_e \gg 1$ and $\omega_{*Te} \gg \omega$. In the weak shear limit, we see that $b_z - k_z b_y/k_y \simeq 1$, and with the conditions $\eta_e \gg 1$ and $\omega \ll \omega_{*Te}$, we may simplify Eq.(2.10) to obtain

$$\tilde{u}_{e||} \simeq \frac{k_{||}}{\omega}\frac{T_e}{m_e n}\tilde{n}_e + \frac{k_{||}}{\omega}\frac{\tilde{T}_e}{m_e} - \frac{e}{m_e c}\left(\frac{k_{||}c}{\omega}\tilde{\Phi} + \frac{\omega_{*Te}}{\omega}\tilde{A}_{||}\right). \quad (2.12)$$

2.2.2 Ion Response

The short-wavelength modes we are considering have characteristic wavelengths much smaller than the ion gyroradius, i.e. $k\rho_{ion} >> 1$, and thus, we may assume an adiabatic ion response. This allows us the following quasineutrality condition:

$$\tilde{n}_e \simeq \tilde{n}_i \simeq -\frac{en}{T_i}\tilde{\Phi}. \tag{2.13}$$

Using quasineutrality, we may eliminate $\tilde{n}_e$ in Eq.(2.12) and find

$$\tilde{u}_{e||} \simeq \frac{k_{||}}{\omega}\frac{\tilde{T}_e}{m_e} - \frac{e}{m_e c}\left(\frac{k_{||}c}{\omega}(1+\tau)\tilde{\Phi} + \frac{\omega_{*Te}}{\omega}\tilde{A}_{||}\right) \tag{2.14}$$

where we have introduced the parameter $\tau \equiv T_e/T_i$.

2.2.3 Perpendicular Momentum Conservation

To determine the perpendicular component of the electron momentum, we linearize Eq.(2.2b) and take its cross product with $\mathbf{b}$ to obtain

$$m_e n\Omega_e \tilde{\mathbf{u}}_{e\perp} = -\mathbf{b}\times\nabla(nT_e) - \mathbf{b}\times\nabla(\tilde{n}T_e) - \mathbf{b}\times\nabla(n\tilde{T}_e) - en\mathbf{b}\times\tilde{\mathbf{E}} + i\omega m_e n\mathbf{b}\times\mathbf{u}_e \tag{2.15}$$

where $\Omega_e = \frac{eB}{m_e c}$ is the electron gyrofrequency. Considering modes with frequencies much slower than the gyrofrequency, $\omega \ll \Omega_e$, we may ignore the last term in Eq.(2.15). We recall now that $\tilde{\mathbf{E}} = -\nabla\tilde{\Phi} - \frac{1}{c}\frac{\partial\tilde{\mathbf{A}}}{\partial t}$ where $|\tilde{\mathbf{A}}_\perp| \ll \tilde{A}_{||}$ in the low-β limit, and also that equilibrium quantities vary only in x. With these considerations, Eq.(2.15) becomes

$$\tilde{\mathbf{u}}_{e\perp} \simeq -\frac{c}{eB}\frac{dT_e}{dx}\left(1+\frac{1}{\eta_e}\right)\tilde{\mathbf{b}}\times\hat{\mathbf{x}} - \frac{c}{eB}\frac{dT_e}{dx}\left(\frac{\tilde{n}_e}{n} + \frac{\tilde{T}_e}{T_e}\frac{1}{\eta_e}\right)\mathbf{b}\times\hat{\mathbf{x}} \tag{2.16}$$

$$- \frac{T_e}{n}\frac{c}{eB}\mathbf{b}\times\nabla\tilde{n}_e - \frac{c}{eB}\mathbf{b}\times\nabla\tilde{T}_e + \frac{c}{B}\mathbf{b}\times\nabla\tilde{\Phi}. \tag{2.17}$$

Here, we use the quasineutrality condition in Eq.(2.13) to replace $\tilde{n}_e$ with $\tilde{\Phi}_e$ in Eq.(2.17), and expanding the vector cross products such that $b_z - k_z b_y/k_y \simeq 1$ and

$\tilde{\mathbf{b}} \times \hat{\mathbf{x}} \simeq \frac{1}{B}\frac{\partial \tilde{A}_{||}}{\partial x}\hat{\mathbf{z}}$, we find

$$\tilde{\mathbf{u}}_{e\perp} \simeq ik_y \frac{c}{B}\left[\frac{1}{e}\tilde{T}_e - (1+\tau)\tilde{\Phi}\right]\hat{\mathbf{x}} \tag{2.18}$$

$$- \frac{c}{B}\left[\frac{1}{e}\frac{d\tilde{T}_e}{dx} + \frac{1}{eT_e}\frac{dT_e}{dx}\frac{1}{\eta_e}\tilde{T}_e - \frac{1}{T_i}\frac{dT_e}{dx}\tilde{\Phi} - (1+\tau)\frac{d\Phi}{dx}\right]\hat{\mathbf{y}} \tag{2.19}$$

$$+ \frac{b_y c}{B}\left[\frac{1}{e}\frac{d\tilde{T}_e}{dx} - (1+\tau)\frac{d\tilde{\Phi}}{dx} - \frac{c}{eB}\frac{dT_e}{dx}\left(1+\frac{1}{\eta_e}\right)\frac{1}{B}\frac{\partial \tilde{A}_{||}}{\partial x}\right]\hat{\mathbf{z}}. \tag{2.20}$$

2.2.4 Ampere's Law

To eliminate $\tilde{u}_{e||}$ in Eq.(2.14), we consider Ampere's law with current supplied by the electrons.

$$\nabla \times \mathbf{B} = -\frac{4\pi ne}{c}\mathbf{u}_e \tag{2.21}$$

Taking the scalar product of Eq.(2.21) with $\mathbf{b}$ to obtain an equation for the parallel component and then linearizing yields

$$\mathbf{b}\cdot\nabla\times\mathbf{B} + \mathbf{b}\cdot\nabla\times\tilde{\mathbf{B}} = -\frac{4\pi ne}{c}\tilde{u}_{e||} \tag{2.22}$$

We have the identity $\nabla\times\nabla\times\tilde{\mathbf{A}} = \nabla(\nabla\cdot\tilde{\mathbf{A}}) - \nabla^2\tilde{\mathbf{A}}$. In the Coulomb gauge, we have $\nabla\cdot\tilde{A} = 0$. Also, $\nabla^2\mathbf{b} \sim \mathbf{b}/L_s^2$ which is small, so we may move $\mathbf{b}$ inside $\mathbf{b}\cdot\nabla^2\tilde{\mathbf{A}}$. We also note that $\nabla\times\mathbf{B} = \frac{B_0}{L_s}\hat{\mathbf{z}}$. With these considerations, we may write Eq.(2.22) as

$$\left[\frac{d^2}{dx^2} - k_y^2\left(1+\frac{k_z^2}{k_y^2}\right)\right]\tilde{A}_{||} \simeq \frac{4\pi ne}{c}\tilde{u}_{e||} \tag{2.23}$$

Given the short transverse scales we are considering, we may take the limit $\frac{k_z^2}{k_y^2} \ll 1$ which yields

$$\left[\frac{d^2}{dx^2} - k_y^2\right]\tilde{A}_{||} \simeq \frac{4\pi ne}{c}\tilde{u}_{e||} \tag{2.24}$$

Eliminating $\tilde{u}_{e||}$ with Eq.(2.14) yields

$$d_e^2\left[\frac{d^2}{dx^2} - k_y^2\right]\tilde{A}_{||} \simeq \frac{k_{||}c}{\omega}\frac{\tilde{T}_e}{e} - \frac{k_{||}c}{\omega}(1+\tau)\tilde{\Phi} - \frac{\omega_{*Te}}{\omega}\tilde{A}_{||} \tag{2.25}$$

where we have introduced the electron plasma frequency, ω_{pe}, given by

$$\omega_{pe}^2 \equiv \frac{4\pi n e^2}{m_e}$$

and the electron skin depth, d_e, given by

$$d_e^2 \equiv \frac{c^2}{\omega_{pe}^2}.$$

2.2.5 Electron Mass Conservation

Linearizing Eq.(2.2a) and expanding the flow divergence yields

$$-i\omega\tilde{n}_e + n\nabla\cdot\tilde{\mathbf{u}}_e + \tilde{u}_{ex}\frac{dn}{dx} = 0. \tag{2.26}$$

Using the quasineutrality condition in Eq.(2.13) and separating $\tilde{\mathbf{u}}_e$ into parallel and perpendicular components as $\tilde{\mathbf{u}}_e = \tilde{u}_{e||}\mathbf{b} + \tilde{\mathbf{u}}_{e\perp}$, we find

$$i\omega\frac{e}{T_i}\tilde{\Phi} + \mathbf{b}\cdot\nabla\tilde{u}_{e||} + \tilde{u}_{e||}\nabla\cdot\mathbf{b} + \nabla\cdot\tilde{\mathbf{u}}_{e\perp} + \tilde{u}_{ex}\frac{1}{n}\frac{dn}{dx} \simeq 0 \tag{2.27}$$

In the limit in which $\frac{\nabla\cdot\mathbf{b}}{k_{||}} \ll 1$, we may eliminate $\tilde{u}_{e||}$ with Eq.(2.24) to arrive at

$$i\omega\frac{e}{T_i}\tilde{\Phi} + i\frac{ck_{||}}{\omega_{pe}^2}\frac{e}{m_e}\left[\frac{d^2}{dx^2} - k_y^2\right]\tilde{A}_{||} + \nabla\cdot\tilde{\mathbf{u}}_{e\perp} + \tilde{u}_{ex}\frac{1}{n}\frac{dn}{dx} \simeq 0. \tag{2.28}$$

To eliminate the divergence term in Eq.(2.28), we refer to the expression for $\tilde{\mathbf{u}}_{e\perp}$ given in Eq.(2.20) and take its divergence. This yields

$$\nabla\cdot\tilde{\mathbf{u}}_{e\perp} = i\frac{\omega_{*Te}}{T_e}\frac{1}{\eta_e}\tilde{T}_e. \tag{2.29}$$

Replacing the divergence term in Eq.(2.28), we obtain

$$\frac{ck_{||}}{\omega_{pe}^2}\frac{e}{m_e}\left[\frac{d^2}{dx^2} - k_y^2\right]\tilde{A}_{||} \simeq -\omega\frac{e}{T_i}\tilde{\Phi} - \frac{\omega_{*Te}}{T_e}\frac{1}{\eta_e}\tilde{T}_e + i\tilde{u}_{ex}\frac{1}{n}\frac{dn}{dx} \tag{2.30}$$

2.2.6 Heat Transport

Linearizing Eq.(2.2c) in the limit in which the temperature gradient dominates the density gradient ($\eta_e \gg 1$) yields

$$\tilde{T}_e \simeq -\frac{i}{\omega}\frac{dT_e}{dx}\tilde{u}_{ex}. \tag{2.31}$$

Noting from Eq.(2.15) that the electric field contributes the dominant force term, we take $\tilde{u}_{ex}$ to be the x-component of the $\mathbf{E} \times \mathbf{B}$ drift. Thus, we have

$$\tilde{u}_{ex} = -i\frac{k_y c}{B}(1+\tau)\tilde{\Phi} \tag{2.32}$$

and from Eq.(2.31), we derive

$$\tilde{T}_e \simeq (1+\tau)\frac{\omega_{*Te}}{\omega}e\tilde{\Phi}. \tag{2.33}$$

Given that we now have relations for both $\tilde{u}_{ex}$ and $\tilde{T}_e$ in terms of $\tilde{\Phi}$, we may solve Eq.(2.30) for $\tilde{\Phi}$ in terms of $\tilde{A}_{||}$. In the limit $\eta_e \gg 1$, we find

$$\tilde{\Phi} \simeq -\frac{ck_{||}}{\omega}\frac{c_{se}^2}{c^2}d_e^2\left[\frac{d^2}{dx^2} - k_y^2\right]\tilde{A}_{||} \tag{2.34}$$

where we have introduced the electron sound velocity

$$c_{se}^2 \equiv \frac{T_i}{m_e}.$$

Since we have all relations in terms of $\tilde{A}_{||}$, we may eliminate all other variables from Eq.(2.25) and taking the limit $\omega_{*Te} \gg \omega$, we find

$$[\omega^3 + k_{||}^2 c_{se}^2 \omega_{*Te}(1+\tau)]d_e^2\left[\frac{d^2}{dx^2} + k_y^2\right]\tilde{A}_{||} + \omega_{*Te}\omega^2\tilde{A}_{||} \simeq 0. \tag{2.35}$$

In the case of weak magnetic shear and slow variation in x, Eq.(2.35) simplifies to

$$d_e^2 k_y^2 \omega^3 - \omega_{*Te}\omega^2 + k_{||}^2 c_{se}^2 \omega_{*Te}(1+\tau)d_e^2 k_y^2 \simeq 0 \tag{2.36}$$

which is the cubic dispersion relation in the fluid limit [4].

Chapter 3

Kinetic Theory

In this chapter, we explore a kinetic treatment [2] of the problem described in section 2.2. At higher-temperatures, as particle mean-free-paths lengthen and the "caging effect" supplied by collisions and the confining field weakens, the fluid model loses validity while kinetic effects become significant. The central region of the plasma column is essentially collisionless, and for the particular modes we are studying, a kinetic treatment provides a more general solution to the problem posed in chapter 2.

3.1 Phase Space

We recall here the distribution function $f(\mathbf{x}, \mathbf{v}, t)$ which describes the distribution of particles in position-velocity space at a given time. More explicitly, the number of particles within the spatial volume element d^3x located at $\mathbf{x}$ and with velocities contained in the velocity volume element d^3v at $\mathbf{v}$ at time t is given by $f(\mathbf{x}, \mathbf{v}, t)d^3xd^3v$. In general, collisions lead to sharp changes in the phase space distribution over short time intervals. In the collisionless limit then, particles flow continuously between regions of phase space, and the distribution f is well-behaved in time. As a result, we may now write a continuity equation for f as follows:

$$\frac{\partial f}{\partial t} + \nabla_{\mathbf{x},\mathbf{v}} \cdot (f\mathbf{U}) = 0 \tag{3.1}$$

where $\mathbf{U}$ is the six-dimensional (*six-vector*) velocity vector $\mathbf{U} = (\dot{\mathbf{x}}, \dot{\mathbf{v}}) = (\mathbf{v}, \frac{\mathbf{F}}{m})$, and $\nabla_{\mathbf{x},\mathbf{v}}$ is the six-dimensional del operator $\nabla_{\mathbf{x},\mathbf{v}} = (\nabla_{\mathbf{x}}, \nabla_{\mathbf{v}})$. To simplify notation, we write $\nabla \equiv \nabla_{\mathbf{x}}$. Now we may expand the divergence term in Eq.(3.1) and obtain

$$\frac{\partial f}{\partial t} + \nabla \cdot (f\mathbf{v}) + \frac{\mathbf{F}}{m} \cdot \nabla_{\mathbf{v}} f + f\frac{\nabla_{\mathbf{v}} \cdot \mathbf{F}}{m} = 0. \tag{3.2}$$

Provided $\mathbf{F}$ does not depend on $\mathbf{v}$, then $\nabla_{\mathbf{v}} \cdot \mathbf{F} = 0$, and the last term drops out of Eq.(3.2). This is certainly true for electric forces, and it can be shown that the Lorentz force, $\mathbf{F}_L = q(\mathbf{E} + \mathbf{v} \times \mathbf{B})$, satisfies the condition, $\nabla_{\mathbf{v}} \cdot \mathbf{F}_{\mathbf{L}} = 0$, though there is an explicit $\mathbf{v}$ dependence in the magnetic force term. In the case of a plasma acted upon by electric and magnetic fields, i.e. $\mathbf{F} = \mathbf{F}_L$, and noting $\nabla \cdot \mathbf{v} = 0$, we obtain the Vlasov equation:

$$\frac{\partial f}{\partial t} + \mathbf{v} \cdot \nabla f + \frac{q}{m}(\mathbf{E} + \mathbf{v} \times \mathbf{B}) \cdot \nabla_{\mathbf{v}} f = 0. \tag{3.3}$$

3.2 Kinetic Effects

For plasma in a strong magnetic field, the gyroradii of individual particles are much smaller than the characteristic length of the field, i.e. $\rho_L \ll L_s$ where ρ_L is the Larmor radius. In that case, we may consider Eq.(3.3) in the guiding center approximation and derive the drift kinetic equation. Decomposing the guiding center motion into motion parallel, $v_{||}\mathbf{b}$, and perpendicular, $\mathbf{v}_{G\perp}$, to the field yields the reduced phase-space equation [2]:

$$\frac{\partial f}{\partial t} + \nabla \cdot \left[\left(\frac{\mathbf{B}}{B} v_{||} + \mathbf{v}_{G\perp} \right) f \right] - \frac{e}{m_e} E_{||} \frac{\partial f}{\partial v_{||}} = 0. \tag{3.4}$$

The perturbed form of (3.4) for an initially plane configuration is given by

$$\frac{\partial \tilde{f}}{\partial t} + v_{||} \frac{\partial \tilde{f}}{\partial x_{||}} + v_{||} \frac{\tilde{B}_x}{B} \frac{\partial f}{\partial x} + \tilde{v}_{Gx} \frac{\partial f}{\partial x} + f \nabla \cdot \tilde{\mathbf{v}}_{G\perp} - \frac{e}{m_e} \tilde{E}_{||} \frac{\partial f}{\partial v_{||}} = 0. \tag{3.5}$$

From the definition of the perturbed magnetic field, we have

$$\tilde{E}_{||} = -ik_{||}\tilde{\Phi} + i\frac{\omega}{c}\tilde{A}_{||}$$

and applying the Coulomb gauge condition, we have

$$\nabla \cdot \tilde{\mathbf{A}} = \nabla_{\perp} \cdot \tilde{\mathbf{A}}_{\perp} + ik_{||}\tilde{A}_{||} = 0.$$

We may now rewrite (3.5) as

$$-i\omega\tilde{f} + ik_{||}v_{||}\tilde{f} + v_{||}ik_y\frac{\tilde{A}_{||}}{B}\frac{\partial f}{\partial x} - ik_y\frac{c\tilde{\Phi}}{B}\frac{\partial f}{\partial x} + i\left(k_{||}\tilde{\Phi} - \frac{\omega}{c}\tilde{A}_{||}\right)\frac{e}{m_e}\frac{\partial f}{\partial v_{||}} = 0 \qquad (3.6)$$

Solving for $\tilde{f}$ in Eq.(3.6) yields

$$\tilde{f} = \frac{e}{m_e c}\left(\frac{k_{||}c\tilde{\Phi} - \omega\tilde{A}_{||}}{\omega - k_{||}v_{||}}\right)\frac{\partial f}{\partial v_{||}} + \frac{e}{T_{||}c}\left(\frac{k_y c D_{||}\tilde{\Phi} - k_y v_{||}D_{||}\tilde{A}_{||}}{\omega - k_{||}v_{||}}\right)\frac{\partial f}{\partial x} \qquad (3.7)$$

where we have introduced a new parameter, $D_{||} \equiv \frac{cT_{||}}{eB}$, which is a measure of diffusion along the field.

We now derive the parallel component of the perturbed flow velocity $\tilde{u}_{||}(\mathbf{x}, t)$ by taking a first moment of $\tilde{f}$ over velocity space as follows:

$$\tilde{u}_{||} = \frac{1}{n}\int_{-\infty}^{+\infty} v_{||}\tilde{f}dv_{||} \qquad (3.8)$$

With Eq.(3.7), we may replace $\tilde{f}$ in Eq.(3.8) with some simplifications to obtain

$$\tilde{u}_{||} = \frac{e}{m_e c}(k_{||}c\tilde{\Phi} - \omega\tilde{A}_{||})\frac{1}{n}\int_{-\infty}^{+\infty}\frac{\omega v_{||}}{\omega^2 - k_{||}^2 v_{||}^2}\left[\frac{\partial f}{\partial v_{||}} + \left(\frac{m_e v_{||}^2}{T_{||}}\right)\frac{k_y D_{||}}{\omega v_{||}}\frac{\partial f}{\partial x}\right]dv_{||}. \qquad (3.9)$$

If we now take the equilibrium distribution as Maxwellian (recall Eq.(2.1)), that is, $f = f_M$, where we have

$$f_M = \frac{n(x)}{[2\pi T_{||}(x)/m_e]^{1/2}}\exp\left[-\frac{m_e v_{||}^2}{2T_{||}(x)}\right], \qquad (3.10)$$

then we may evaluate the derivatives in Eq.(3.9) to find

$$\tilde{u}_{||} \simeq \frac{e}{m_e c}(k_{||} c\tilde{\Phi} - \omega \tilde{A}_{||}) \frac{1}{n} \int_{-\infty}^{+\infty} f_M \left(\frac{m_e v_{||}^2}{T_{||}} \right) \frac{\omega - \omega_{*Te} \hat{\mathcal{L}}(v_{||}^2)}{\omega^2 - k_{||}^2 v_{||}^2} dv_{||} \tag{3.11}$$

where we have simplified $\frac{\partial f}{\partial x}$ in the limit $\eta_e \gg 1$ and introduced the function

$$\hat{\mathcal{L}}(v_{||}^2) = \frac{m_e v_{||}^2}{2T_{||}} - \frac{1}{2}.$$

We now consider mode frequencies in the limit $\omega^2 \gg k_{||}^2 v_{th}^2$. Again, we consider modes in which the ion gyroradius is large and we may assume an adiabatic ion response. Then we may apply the quasineutrality condition to find

$$\tilde{\Phi} \simeq -\frac{T_i}{e} \frac{k_{||} \tilde{u}_{e||}}{\omega} \tag{3.12}$$

and using Eq.(3.12) in Eq.(3.11), we obtain

$$\tilde{u}_{||} \simeq \frac{e}{m_e c} \left[1 - \frac{k_{||}^2 c_{se}^2 \Omega_*}{\omega^3} \right]^{-1} \frac{\Omega_*}{\omega} \tilde{A}_{||} \tag{3.13}$$

where we have defined a new parameter, Ω_*, to express the integral in Eq.(3.11).

$$\Omega_* \equiv \frac{\omega^2}{n} \int_{-\infty}^{+\infty} f_M \left(\frac{m_e v_{||}^2}{T_{||}} \right) \frac{\omega_{*Te} \hat{\mathcal{L}}(v_{||}^2) - \omega}{\omega^2 - k_{||}^2 v_{||}^2} dv_{||}. \tag{3.14}$$

Recalling Ampere's Law as given in Eq.(2.24), we eliminate $\tilde{u}_{||}$ in Eq.(3.13), we find

$$d_e^2 \left[\frac{d^2}{dx^2} - k_y^2 \right] \tilde{A}_{||} \left[1 + \frac{\Omega_* k_{||}^2 c_{se}^2}{\omega^3} \right] \simeq -\frac{\Omega_*}{\omega} \tilde{A}_{||}. \tag{3.15}$$

Note that in the limit given by $k_{||}^2 v_{||}^2 \ll \omega^2 \ll \omega_{*Te}^2$, we find that $\Omega_* \simeq \omega_{*Te}$, and we recover the cubic dispersion relation from Eq.(2.36) up to a constant factor ~ 1.

Chapter 4

Analysis of Micro-Reconnecting Modes

In this chapter, we investigate in detail the micro-reconnecting mode identified in chapters 2 and 3. In particular, we derive the dispersion relation [3] and examine mode stability. We also consider an approximation to the dispersion relation in the fluid limit.

4.1 Dispersion Relation

To simplify notation, we define the wave number

$$k \equiv k_y$$

and the dimensionless integral parameter

$$\mathcal{F}_0^0 \equiv \frac{\Omega_*}{\omega_{*Te}}.$$

Recalling Eq.(3.15), we derive the following quadratic form:

$$d_e^2 \left\langle \left| \frac{d\tilde{A}_{||}}{dx} \right|^2 + k^2 |\tilde{A}_{||}|^2 \right\rangle = \left\langle |\tilde{A}_{||}|^2 \frac{\omega_{*T}\omega^2 \mathcal{F}_0^0}{\omega^3 + k_{||}^2 c_{se}^2 \omega_{*T} \mathcal{F}_0^0} \right\rangle \tag{4.1}$$

where brackets denote integration over the dimension of variation

$$\langle\ \rangle \equiv \int_{-\infty}^{+\infty} dx.$$

To simplify Eq.(4.1) and the integral for $\mathcal{F}_0^0$, we define the following quantities: the electron thermal velocity, v_{the}, and the fluid parameter, U:

$$v_{the}^2 = \frac{2T_{||}}{m_e} \equiv \frac{c_{se}^2}{2}$$
$$U \equiv \frac{k_{||}^2 v_{the}^2}{\omega_{*T}^2}$$

The parameter U expresses the fluid character of the plasma where $U \ll 1$ indicates the fluid limit. With these definitions, $\mathcal{F}_0^0$ takes the following form:

$$\mathcal{F}_0^0 = \frac{1}{\sqrt{\pi}} \int_{-\infty}^{+\infty} d\zeta \left[\exp(-\zeta^2)\right] 2\zeta^2 \frac{\mathcal{L}(\zeta^2) - \bar{\omega}}{1 - \frac{U}{\bar{\omega}^2}\zeta^2} \tag{4.2}$$

where

$$\mathcal{L}(\zeta^2) = \zeta^2 - \frac{1}{2}.$$

The kinetic integral, $\mathcal{F}_0^0$, describes integration over the velocity parameter, $v_{||}$, and therefore includes the effects of Landau resonances. Given weak magnetic shear and that the equilibrium quantities vary slowly in x, we may write

$$k_{||} \cong k_z$$
$$\left|\frac{\partial^2}{\partial x^2}\right| \ll k_y^2$$

Simplifying Eq.(4.1), we obtain

$$k^2 d_e^2 \simeq \frac{\omega_{*T}\omega^2 \mathcal{F}_0^0}{\omega^3 + k_{||}^2 v_{si}^2 \omega_{*T} \mathcal{F}_0^0}. \tag{4.3}$$

Introducing the following rescaled variables,

$$\bar{\omega} \equiv \frac{\omega}{\omega_{*Te}}$$
$$\bar{k}_e \equiv k d_e$$

the equation to be solved is

$$\frac{1}{\mathcal{F}_0^0}\bar{\omega}^3 - \frac{\bar{\omega}^2}{\bar{k}_e^2} + \frac{1}{2}U = 0. \tag{4.4}$$

4.2 Limiting Case

In the limit of $U \to 0$ (ideal fluid limit), we may evaluate the integral in Eq.(4.2) using the identity $\int_{-\infty}^{\infty} \exp(-t^2)t^{2z}dt = \Gamma(\frac{z+1}{2})$. In the limit $U \to 0$, we find $\mathcal{F}_0^0 \simeq 1$, and Eq.(4.4) reduces to the cubic in Eq.(2.36). In this limit, then, we examine the following equation

$$f(\bar{\omega}) = \bar{\omega}^3 - \frac{\bar{\omega}^2}{\bar{k}_e^2} + \frac{1}{2}U = 0. \tag{4.5}$$

From the properties of cubics, we note that $f(\bar{\omega}) = 0$ has at least one real root for $U > 0$ and at most three depending on the value of the parameters $\bar{k}_e$ and U. Graphs of $f(\bar{\omega})$ for various U and $\bar{k}_e^2 = 1.5$ is shown in Figure 4-1. We would like to determine the conditions at which the roots of f transition from real to complex. First, we consider the cubic discriminant, Δ, given by the following:

$$\Delta = -\frac{2}{\bar{k}_e^6}U + \frac{27}{4}U^2. \tag{4.6}$$

For $\Delta < 0$, Eq.(4.5) has three, distinct, real roots. For $\Delta > 0$, two of the roots are complex and conjugate. Thus, the transition occurs at $\Delta = 0$, and this gives the condition

$$U_c = \frac{1}{\bar{k}_e^6}\frac{8}{27} \tag{4.7}$$

for $U = U_c$ at the transition point.

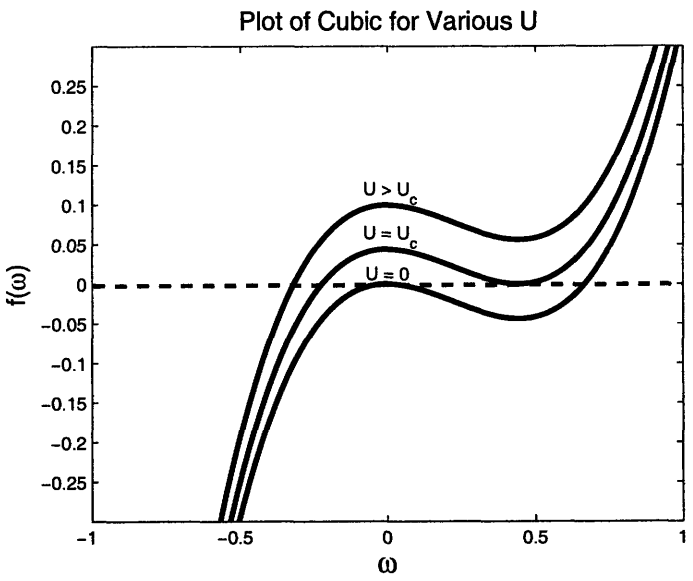

Figure 4-1: Graphs of $f(\bar{\omega})$ with $\bar{k}_e^2 = 1.5$ shown for $U = 0$, $U = U_c$ (critical value), and $U > U_c$.

Alternatively, we now consider the first derivative of f to find its local minimum:

$$f'(\bar{\omega}) = 3\bar{\omega}^2 - \frac{2\bar{\omega}}{\bar{k}_e^2}. \tag{4.8}$$

It is clear that f achieves a local maximum at $\bar{\omega}_{max} = 0$, and we take the second root of Eq.(4.8), $\bar{\omega}_{min} = \frac{2}{3\bar{k}_e^2}$, to be the local minimum. Now the critical value of U at the point of transition can be determined by solving $f(\bar{\omega}_{min}) = 0$ for U. We find this value to be

$$U = U_c = \bar{\omega}_{min}^3 \tag{4.9}$$

where U_c is the value given in Eq.(4.7). The trajectory of the roots in the complex plane for increasing U is shown in Figure 4-2.

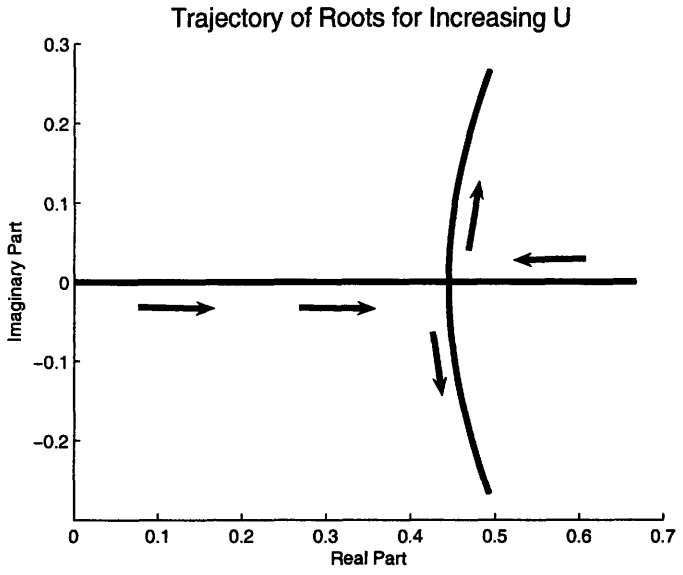

Figure 4-2: Trajectory of roots of Eq.(4.5) which become complex as U increases from 0. Arrows indicate motion of roots.

4.3 General Case

Returning to the general case of U small, but finite, we define new variables:

$$\bar{\omega}_0 \equiv \frac{\bar{\omega}}{U^{1/3}}$$
$$\bar{k}_0^2 \equiv \frac{U^{1/3}}{U_c^{1/3}}.$$

This rescaling complicates the physical interpretation of our results as we will see in the next section, but we sacrifice transparency for computational simplicity. With the definitions of $\bar{\omega}_0$ and $\bar{k}_0$, Eq.(4.4) becomes

$$\frac{1}{\mathcal{F}_0^0}\bar{\omega}_0^3 - \frac{3}{2}\frac{\bar{\omega}_0^2}{\bar{k}_0^2} + \frac{1}{2} = 0 \tag{4.10}$$

and Eq.(4.2) becomes

$$\mathcal{F}_0^0 = \frac{1}{\sqrt{\pi}}\int_{-\infty}^{+\infty} d\zeta \exp\left[-\zeta^2\right] 2\zeta^2 \frac{\mathcal{L}(\zeta^2) - U^{1/3}\bar{\omega}_0}{1 - \frac{U^{1/3}}{\bar{\omega}_0^2}\zeta^2}. \tag{4.11}$$

Besides yielding simpler equations, the definition of $\bar{k}_0$ has the useful interpretation of characterizing the roots of Eq.(4.4) in the limit of $U \to 0$. The condition $\bar{k}_0^2 > 1$ gives the possibility of complex solutions to Eq.(4.10), and this possibility will now be investigated.

4.4 Numerical Analysis

Here, we would like to determine values of $\bar{\omega}_0$ that simultaneously satisfy both Eq.(4.10) and Eq.(4.11) given values of $\bar{k}_0$ and U. In particular, we are interested in finding complex values of $\bar{\omega}_0$ in the first quadrant of the complex plane, as values for ω in Eq.(2.4) with positive imaginary parts indicate unstable modes. To evaluate the integral in Eq.(4.11), we define the parameter $\epsilon \equiv U^{1/3}$, and in terms of ϵ, the integral becomes

$$I(\epsilon) = \frac{1}{\sqrt{\pi}} \int_{-\infty}^{+\infty} d\zeta \exp\left[-\zeta^2\right] 2\zeta^2 \frac{\mathcal{L}(\zeta^2) - \epsilon\bar{\omega}_0}{1 - \frac{\epsilon}{\bar{\omega}_0^2}\zeta^2}. \tag{4.12}$$

Here, we present the results of a code written in Mathematica which solves for $\bar{\omega}_0$ given values for $\bar{k}_0^2$ and ϵ. Trajectories of complex values of $\bar{\omega}_0$ satisfying Eq.(4.10) and Eq.(4.11) in the first quadrant for fixed values of $\bar{k}_0$ and increasing ϵ are depicted in Figure 4-3. The trajectories cross as a result of the scaling $\bar{\omega}_0 \equiv \frac{\bar{\omega}}{U^{1/3}}$ and $\bar{k}_0^2 \equiv \frac{U^{1/3}}{U_c^{1/3}}$. The parameters $\epsilon = U^{1/3}$ and $\bar{k}_0^2$ are not independent in the sense that $\bar{k}_e^2 = \frac{2}{3}U_c^{-1/3}$ must vary inversely with ϵ in order to hold $\bar{k}_0^2$ fixed. We note that as ϵ increases, the growth rate given by the imaginary part of $\bar{\omega}_0$ goes to 0, which is what we would expect for decreasing $\bar{k}_e^2$.

4.5 Approximation of $\mathcal{F}_0^0$

We would now like to approximate the integral in Eq.(4.12) in the case in which ϵ is small and $\bar{\omega}_0$ is in the first quadrant of the complex plane (positive real and imaginary parts). Defining a new parameter, $\xi \equiv \frac{\epsilon}{\bar{\omega}_0^2}$, we see that ξ has a negative imaginary

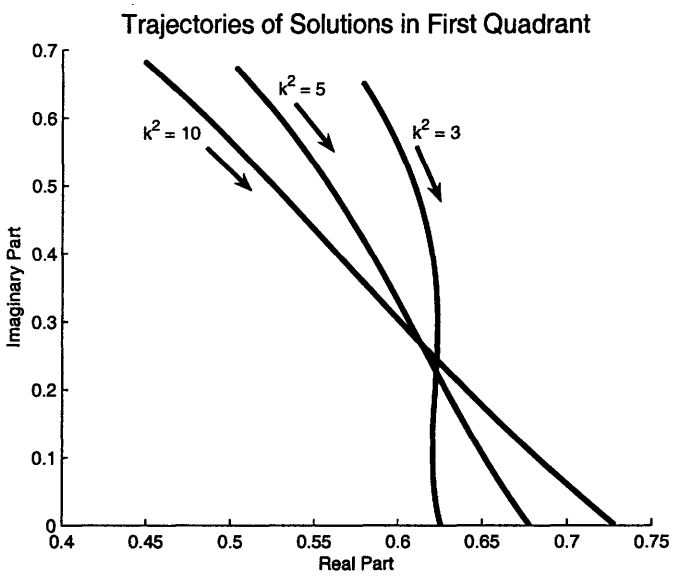

Figure 4-3: Trajectories of first-quadrant solutions for $\bar{\omega}_0$ in Eq.(4.10) for ϵ increasing from 10^{-3}. Arrow indicates direction of increasing ϵ. Trajectories are plotted for $\bar{k}_0^2 = 3$, 5, and 10.

part when $\bar{\omega}_0$ is in the first quadrant. Writing the integral for $\mathcal{F}_0^0$ in terms of ξ yields,

$$I = \frac{1}{\sqrt{\pi}} \int_{-\infty}^{+\infty} \exp\left[-\zeta^2\right] 2\zeta^2 \frac{\mathcal{L}(\zeta^2) - \xi\bar{\omega}_0^3}{1 - \xi\zeta^2} d\zeta. \tag{4.13}$$

Naively, we might first try to approximate I by replacing the denominator with a power series expansion for small $\xi\zeta^2$. Although ζ^2 goes to infinity in the integral, we might hope that the decaying exponential term, $e^{-\zeta^2}$, will suppress the contribution of the large values of ζ^2 for which $|\xi\zeta^2| \gtrsim 1$. Expanding the denominator to second order in ϵ and applying the identity

$$\int_{-\infty}^{\infty} \exp(-t^2) t^{2z} dt = \Gamma(\frac{z+1}{2})$$

to integrate, we obtain

$$\begin{aligned} I &\simeq \frac{1}{\sqrt{\pi}} \int_{-\infty}^{+\infty} \left[\exp(-\zeta^2)\right] 2\zeta^2 (\zeta^2 - \frac{1}{2} - \epsilon\bar{\omega}_0)(1 + \frac{\epsilon}{\bar{\omega}_0^2}\zeta^2 + \frac{\epsilon^2}{\bar{\omega}_0^4}\zeta^4) d\zeta \\ &= \frac{1}{\bar{\omega}_0^2} \left(3\epsilon - \bar{\omega}_0^3\epsilon - \frac{3}{2}\bar{\omega}_0\epsilon^2 + \frac{90}{8}\frac{\epsilon^2}{\bar{\omega}_0^2}\right) + 1. \end{aligned} \tag{4.14}$$

In a more rigorous method, we recall that we are considering complex values of $\bar{\omega}_0$ in the first quadrant. Thus, we may write $\bar{\omega}_0 = re^{i\theta}$ for some real, positive r, and $0 < \theta < \frac{\pi}{2}$. To simplify Eq.(4.13), we use the following identity:

$$\frac{1}{1-\xi\zeta^2} = -i\int_0^\infty \exp\left[is(1-\xi\zeta^2)\right] ds. \tag{4.15}$$

The integral on the RHS converges whenever ξ has a negative imaginary part, and for $\bar{\omega}_0 = re^{i\theta}$ in the first quadrant, we see that $\xi = \frac{\epsilon}{r^2}e^{-i2\theta}$ which is in the fourth quadrant for $\theta < \frac{\pi}{4}$ and in the third quadrant for $\theta > \frac{\pi}{4}$. Thus, ξ has a negative imaginary part, and Eq.(4.15) holds. Applying the identity in Eq.(4.13) gives a double integral, and interchanging the order of integration yields the following:

$$I = \frac{1}{\sqrt{\pi}}\int_0^\infty e^{is}\int_{-\infty}^{+\infty} \exp\left[-(1+is\xi)\zeta^2\right] 2\zeta^2(\mathcal{L}(\zeta^2) - \xi\bar{\omega}_0^3) d\zeta ds. \tag{4.16}$$

We note here that the inner integration involves taking the second and fourth moments of a Gaussian distribution which we will express as G_2 and G_4, respectively, according to the following:

$$G_n = \frac{1}{\sigma\sqrt{2\pi}}\int_{-\infty}^{+\infty} x^n \exp\left[-\frac{x^2}{2\sigma^2}\right] dx. \tag{4.17}$$

With a distribution of the form given in Eq.(4.17), we find $G_2 = \sigma^2$, and $G_4 = 3\sigma^4$. With these moments, the double integral in Eq.(4.13) simplifies to

$$I = -i\int_0^\infty e^{is}\left[\frac{3}{2}(1+is\xi)^{-5/2} - (\frac{1}{2}+\xi\bar{\omega}_0^3)(1+is\xi)^{-3/2}\right] ds. \tag{4.18}$$

The Fourier-like integral in Eq.(4.18) may be expanded by integrating by parts. Integrating the first term on the RHS of Eq.(4.18), we find

$$\begin{aligned} -i\int_0^\infty e^{is}\frac{3}{2}(1+is\xi)^{-5/2} ds &= -\frac{3}{2}\left[e^{is}(1+is\xi)^{-5/2}\right]_0^\infty - i\xi\frac{15}{4}\int_0^\infty e^{is}(1+is\xi)^{-7/2} ds \\ &= \frac{3}{2} - i\xi\frac{15}{4}\int_0^\infty e^{is}(1+is\xi)^{-7/2} ds. \end{aligned}$$

We note that each integration by parts produces an additional prefactor ξ in front

of the integral remainder. Thus, for $\epsilon \ll 1$, the integral remainders diminish with increasing powers of ξ. If we then integrate Eq.(4.18) by parts and ignore terms of higher order than ϵ^2, we obtain

$$I \simeq 1 + \frac{1}{\bar{\omega}_0^2}\left(3\epsilon - \bar{\omega}_0^3\epsilon + \frac{90}{8}\frac{\epsilon^2}{\bar{\omega}_0^2} - \frac{3}{2}\bar{\omega}_0\epsilon^2\right) \tag{4.19}$$

which is the same approximation we found with our naive expansion of the denominator in Eq.(4.14).

4.6 Verification of Integral Approximation

To check the validity of the approximation for I in Eq.(4.19), we numerically integrated (4.12) in Mathematica for values of ϵ and $\bar{\omega}_0$ in the range $\epsilon \in [10^{-3}, 1]$ and $\bar{\omega}_0 = re^{i\theta}$ with $r = 1$ and $\theta \in (0, \frac{\pi}{2})$. As shown in the following figures, the real (Figure 4-4) and imaginary (Figure 4-5) parts of the resulting values of integration via Mathematica are plotted against ϵ as a solid line, and the real imaginary parts of the values given by the approximation in Eq.(4.19) are plotted as a dashed line.

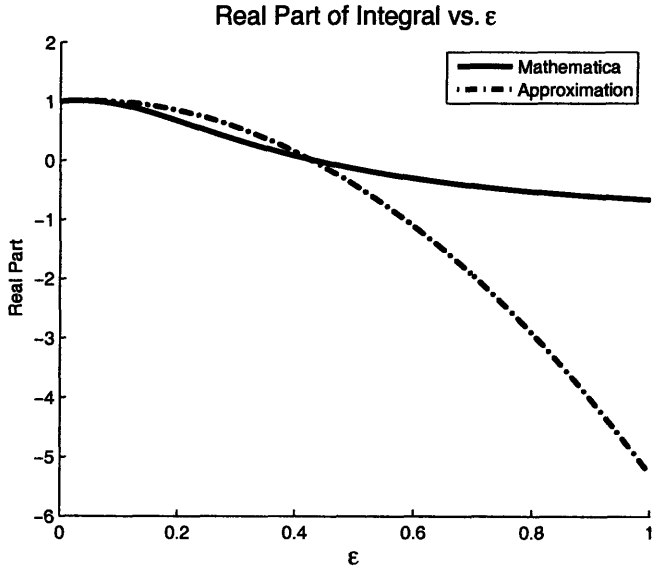

Figure 4-4: Real part of I plotted against ϵ with $\bar{\omega}_0 = e^{i\frac{\pi}{6}}$. Solid line is value of integral given in Eq.(4.11) determined by Mathematica code. Dashed line is value of the approximation given in Eq.(4.19).

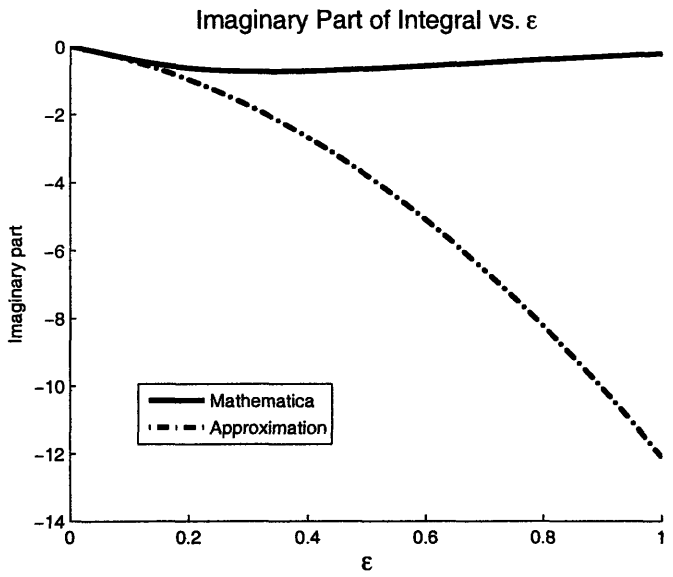

Figure 4-5: Imaginary part of I plotted against ϵ with $\bar{\omega}_0 = e^{i\frac{\pi}{6}}$. Solid line is value of integral given in Eq.(4.11) determined by Mathematica code. Dashed line is value of the approximation given in Eq.(4.19).

4.7 Approximation of Dispersion Relation

Using the approximation for $\mathcal{F}_0^0$ given in Eq.(4.19), we approximate the dispersion relation in Eq.(4.10) by the following septic equation:

$$(1+q\epsilon)\bar{\omega}_0^7 - q\bar{\omega}_0^6 + \left(\frac{3}{2}q\epsilon^2 - \frac{1}{2}\epsilon\right)\bar{\omega}_0^5 + \left(\frac{1}{2} - 3q\epsilon\right)\bar{\omega}_0^4 - \frac{3}{4}\epsilon^2\bar{\omega}_0^3 + (\frac{3}{2}\epsilon - \frac{45}{4}q\epsilon^2)\bar{\omega}_0^2 + \frac{45}{8}\epsilon^2 = 0 \quad (4.20)$$

where $q = \frac{3}{2k_0^2}$. To examine the validity of the approximation, we compare the trajectory of the solution to the septic equation against the trajectories in Figure 4-3. A comparison over the range over the range $\epsilon \in [10^{-3}, \frac{1}{20}]$ is shown in Figure 4-6.

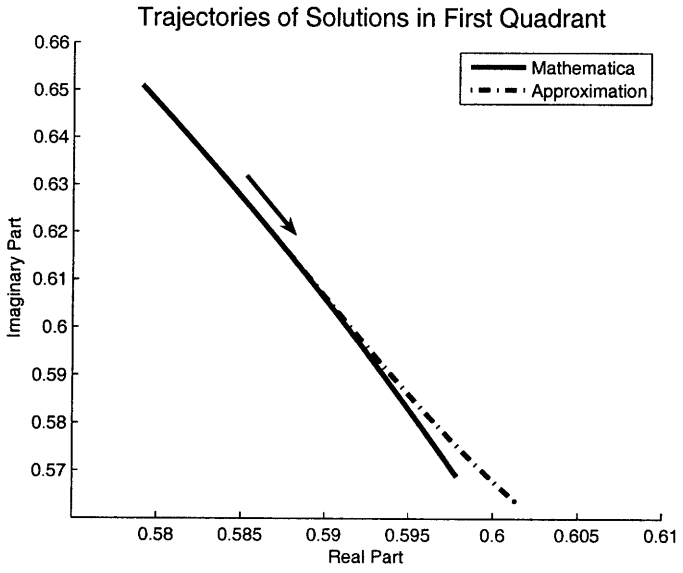

Figure 4-6: Plot of trajectory of solution to Eq.(4.10) determined with Mathematica code compared with trajectory of solution to Eq.(4.20) determined by approximation. Solutions plotted for $\bar{k}_0^2 = 3$ and $\epsilon \in [10^{-3}, \frac{1}{20}]$. Arrow indicates direction of increasing ϵ.

Chapter 5

Conclusions

In summary, we have investigated the stability of micro-reconnecting modes by deriving the dispersion relation in both the fluid and kinetic theory. We found that the results of kinetic theory simplify to the results of fluid theory in the appropriate limit and that the dispersion relation permits unstable values of ω. The further question of whether these background microinstabilities give rise to macroscopic particle transport remains open to investigation. Future work may also approximate the kinetic integral in Eq.(4.2) by making use of Eq.(4.19) derived in section 4.5 for small values of the fluid parameter.

5.1 Future Directions of Research

As we have identified the modes as unstable, we are left with the problem of justifying their interaction with the drift-tearing mode. This problem has been investigated and discussed in [7] and [4]. An immediate extensions of the work in this thesis involves the anomalous transport mentioned in Chapter 1.

In quasilinear theory, linear instabilities give rise to particle transport when density and velocity perturbations are not in phase. The results of Chapter 4 show that there are conditions in which the micro-reconnecting modes are linearly unstable. One clear extension of the work in this thesis would be to use the approximation in Eq.(4.20) to derive a quasilinear estimate of the flow. This value could then be

compared with experimentally measured rates of anomalous transport.

Bibliography

[1] B. Coppi. Collisionless process for particle inward transport. Proposed Letter, 2006.

[2] B. Coppi. Notes on kinetic derivation of micro-reconnecting modes. Notes on work to be published, 2006.

[3] B. Coppi. Notes on quadratic form and dispersion relation. Notes on work to be published, 2006.

[4] B. Coppi. Theoretical resolution of magnetic reconnection in high energy plasmas. In *Collective Phenomena in Macroscopic Systems.* Publ. World Scientific, 2007.

[5] B. Coppi and C. Spight. Ion-mixing mode and model for density rise in confined plasmas. *Phys. Rev. Lett.*, 41(8):551, 1978.

[6] C. Crabtree. Notes on fluid derivation of micro-reconnecting modes. Notes on work to be published, 2006.

[7] B. Coppi et.al. Interaction of drift-tearing (mesoscopic) modes with coherent and turbulent microscopic structures. In *International Atomic Energy Agency Proceedings Series*, 2006.

[8] R.J. Goldston and P.H. Rutherford. *Introduction to Plasma Physics.* Institute of Physics Publishing, 1997.

[9] K. Miyamoto. *Plasma Physics for Nuclear Fusion.* MIT Press, 1989.

[10] K. Nishikawa and M. Wakatani. *Plasma Physics.* Springer-Verlag, 1993.